POLSKA AKADEMIA NAUK
Instytut Badań Systemowych

ESSAYS ON STABILITY ANALYSIS AND MODEL REDUCTION

Umberto Viaro

Warsaw 2010

SYSTEMS RESEARCH INSTITUTE
POLISH ACADEMY OF SCIENCES
Series: SYSTEMS RESEARCH
Volume 68

Series Editor:

Prof. Jakub Gutenbaum

Warsaw 2010

SYSTEMS RESEARCH INSTITUTE
POLISH ACADEMY OF SCIENCES

==========

Umberto Viaro

ESSAYS ON STABILITY ANALYSIS AND MODEL REDUCTION

Warsaw 2010

Prof. Umberto Viaro
Dipartimento di Ingegneria Elettrica, Gestionale e Meccanica
Università degli Studi di Udine
via delle Scienze 208, 33100 Udine, Italy
email: viaro@uniud.it

Preface by Prof. Wiesław Krajewski
Systems Research Institute
Polish Academy of Sciences
01-447 Warsaw, Newelska 6
Wieslaw.Krajewski@ibspan.waw.pl

Papers Reviewers:

Prof. Jerzy Klamka
Prof. Stanisław Bańka

Partially supported by the University of Udine

ISSN 0208-8029

ISBN 9788389475282

Chapter 4

The method of the indifference areas

The digital filters resulting from the implementation of linear time–invariant systems on digital computers or on dedicated hardware are necessarily nonlinear due to the finite wordlength of the processors, which causes signal quantization and overflow [1], [2]. The effect of these nonlinearities is particularly important in the digital filters realized with fixed–point arithmetic that is still used in most low–cost embedded microprocessors and microcontrollers [3]. Even if the internal wordlength is long, so that the digital filter "approaches" the behaviour of its linear prototype, undesirable phenomena arise, such as the presence of limit cycles for parameter values that belong to the stability region of the linear prototype. These phenomena are still considered with interest in the recent literature (see, e.g., [4], [5] and bibliographies therein).

Quantization is responsible for small–amplitude limit cycles, whereas large–amplitude limit cycles are due to overflow [6]. Usually, the effects of quantization and overflow can be considered as noninteracting [7]. The occurrence and form of the cycles depend on the quantization and overflow characteristics as well as on the filter realization (see, e.g., [8]). Since digital filters are often realized as a single second–order unit or as a cascade or parallel of second–order cells, a large part of the literature deals with them. This chapter focuses on second–order filter sections, too. In particular, it concentrates on the quantization effets in direct–form filters with the quantizers located after each multiplication or after summation. The purpose is to determine the regions of the parameter

plane where such filters are globally asymptotically stable and where they exhibit zero–input limit cycles of given period and amplitude. It turns out that the method of the indifference areas, illustrated in [9] for the case of two quantizers (one after each multiplier) and in [10] for that of one quantizer (after the adder), is more effective than the general method suggested in [11] since it allows us to find the *entire* parameter region where the filter is globally asymptotically stable, as well as the whole existence area of a given cycle [12].

Section 4.1 briefly recalls the filter equations. Section 4.2 derives bounds on the possible cycle amplitude depending on the adopted quantization characteristic. Based on these bounds, Section 4.3 shows how the parameter plane can be partitioned into regions whose points are characterized by the same filter behaviour, and Section 4.4 determines the entire region where the filter is globally asymptotically stable. A procedure to find the region supporting a given cycle is outlined in Section 4.5. Some concluding remarks are drawn in Section 4.6.

4.1 Direct–form filters

The direct–form state equations of the linear prototype of a second–order filter are:

$$x_1(n) = x_2(n-1)\,, \tag{4.1}$$

$$x_2(n) = ax_2(n-1) + bx_1(n-1) + u(n). \tag{4.2}$$

Assuming $u(n) = 0, \forall n$, the unforced evolution of the output $y(n) = x_2(n)$ is described by the recurrence relation:

$$y(n) = ay(n-1) + by(n-2). \tag{4.3}$$

In the plane of parameters a and b, the stability region is the triangle ABC of Figure 4.1. In fact, for parameter values inside this triangle the poles of the filter transfer function:

$$H(z) = \frac{z^2}{z^2 - az - b} \tag{4.4}$$

are inside the unit circle centred at the origin of the z–plane.

The homogeneous equation of the corresponding digital filter output with the quantizers placed after each multiplication is

$$y(n) = [ay(n-1)]_Q + [by(n-2)]_Q\,, \tag{4.5}$$

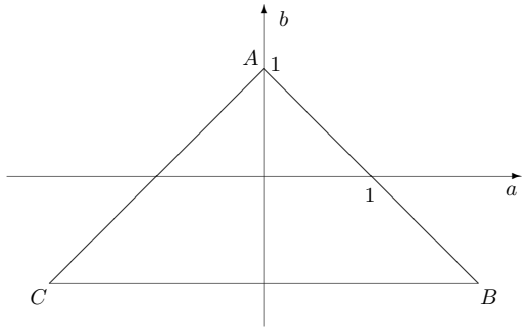

(a)

Figure 4.1: Stability regions for the linear prototype.

whereas the equation of the digital filter output with the quantizer placed after summation is

$$y(n) = [ay(n-1) + by(n-2)]_Q \,, \tag{4.6}$$

where $[\cdot]_Q$ denotes quantization. By normalizing the quantization step q to unity, $y(n) \in \mathbb{Z}$, $\forall n$ (integer arithmetic).

The free response of (4.5) or (4.6) can be expressed as the response of the associated linear filter to a fictitious input $u(n) = e(n)$:

$$y(n) = ay(n-1) + by(n-2) + e(n), \tag{4.7}$$

where

$$e(n) = [ay(n-1)]_Q - ay(n-1) + [by(n-2)]_Q - by(n-2) \tag{4.8}$$

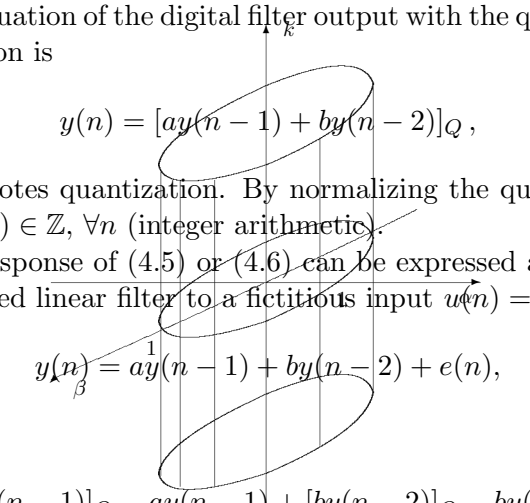

(b)

or, respectively,

$$e(n) = [ay(n-1) + by(n-2)]_Q - ay(n-1) - by(n-2) \tag{4.9}$$

is the quantization error. For example, the value of $|e(n)|$ for (4.8) satisfies the inequality:

$$|e(n)| < 1 \tag{4.10}$$

in the case of roundoff quantization, the inequality:

$$|e(n)| < 2 \tag{4.11}$$

in the case of magnitude truncation quantization, and the inequality:

$$|e(n)| \leq 2 \tag{4.12}$$

in the case of value (or two's complement) truncation quantization (see p. 45 of [13]).

4.2 Bounds on the cycle amplitude

If the linear filter is asymptotically stable, its free response tends to zero. Its forced (or driven) response $y_d(n)$ to the bounded input $e(n)$ is also bounded. Precisely, $y_d(n)$ is given by

$$y_d(n) = h(n) * e(n), \tag{4.13}$$

where $h(n)$ denotes the unit–sample response and $*$ denotes convolution. It follows that, in the case of roundoff and magnitude truncation, the maximum amplitude of the limit cycles, if any, cannot exceed the bound:

$$B = [\sup_n |e(n)|] \cdot \Sigma_n |h(n)| \tag{4.14}$$

and, in the case of value truncation, the bound:

$$B = [\sup_n |e(n)|]\, S, \tag{4.15}$$

with

$$S := \sup \{\Sigma_n\, h_+(n), -\Sigma_n\, h_-(n)\}, \tag{4.16}$$

where $h_+(n)$ and $h_-(n)$ denote, respectively, the positive and negative values in the unit–sample response. These bounds can be evaluated numerically or approximated by means of suitable formulae that depend on the parameter values in a simple way (see, e.g., [14]).

To detect all of the zero–input limit cycles, if any, it is therefore enough to consider, for any parameter pair (a, b), the free evolution of the nonlinear filter from the initial conditions $[y(-2), y(-1)]$ satisfying the inequalities:

$$|y(-2)| \leq B, \;\; |y(-1)| \leq B. \tag{4.17}$$

Since the same cycles can be found starting from either

$$|y(-2)| \leq |y(-1)| \leq B \tag{4.18}$$

or

$$|y(-1)| \leq |y(-2)| \leq B, \tag{4.19}$$

the number of free evolutions to be considered is actually less than $4B^2$. This number can be further reduced when the quantization characteristic is symmetric (roundoff and magnitude truncation) because in this case the evolution from $[y(-2), y(-1)]$ is the negative of the evolution from $[-y(-2), -y(-1)]$, so that the analysis can be limited only to the initial conditions satisfying

$$|y(-2)| \leq y(-1) \leq B, \tag{4.20}$$

whose number is about B^2.

4.3 Indifference areas

The signal boundedness induces a quantization of the (a, b)–plane independent of the finite–wordlength representation of the parameters. Precisely, given a parameter region where the output amplitude cannot exceed an upper bound B, this region can be subdivided into a finite number of areas such that all sequences $\{y(n)\}$, with $|y(n)| \leq B$, are the same for all of the points inside the same area and, therefore, only one point for each area need be considered. This is the reason why such areas have been called indifference areas in [9] and [10].

Quantization after multiplication

If the quantizers are placed after each multiplication as in (4.5), the indifference areas are rectangles whose sides are parallel to the coordinate axes [9]. To see this, consider the product ak with k integer and assume that $[\cdot]_Q$ denotes magnitude truncation so that $[ak]_Q = \lfloor |ak| \rfloor \cdot \mathrm{sgn}(ak)$. Then $[ak]_Q$ takes the same integer value at all a–points in an interval of length $1/|k|$; for instance, if $k > 0$ and $a > 0$, $[ak]_Q = i$ for $a \in [i/k, (i+1)/k]$. The same is true for b.

If in a region $\mathcal{R}$ internal to the stability triangle of the linear prototype the upper bound of (4.13) is B, then the minimal partition of the (a, b)–plane that ensures the exhaustive analysis of the nonlinear filter behaviour inside $\mathcal{R}$ is obtained by drawing the horizontal lines $b = i/k$ and the vertical lines $a = i/k$ with $i = 0, \pm 1$ and $k = 1, 2, \ldots, B$ (clearly,

it is enough to consider only positive values of k since the magnitude truncation characteristic is symmetric). In this way, the side length ℓ of the resulting indifference rectangles takes the values:

$$\ell = \left|\frac{h}{l} - \frac{m}{n}\right|, \;\; 0 \le h \le l \le B, \;\; 0 \le m \le n \le B, \tag{4.21}$$

with $\left|\frac{h}{l} - \frac{m}{n}\right| \ge \frac{1}{B(B-1)}$ and $hn - lm \neq 0$. Fig. 4.2 shows the parameter plane partition for the magnitude–truncation quantization after each multiplication and $B = 4$.

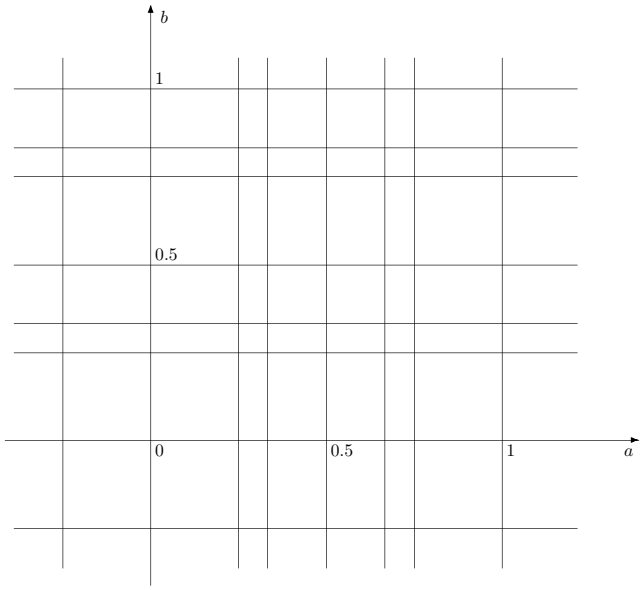

Figure 4.2: Parameter–plane grid for a direct–form filter with magnitude–truncation quantization after each multiplication and $B = 4$.

Similar considerations can be made for the roundoff quantization, even if the number of indifference rectangles corresponding to the same upper bound B increases. Fig. 4.3 shows the parameter partition for the roundoff quantization after each multiplication and $B = 4$.

A little more complex is the case of two's complement truncation because of the asymmetry of the quantization characteristic: in particular, it is not possible to associate a side to either of the adjacent rectangles,

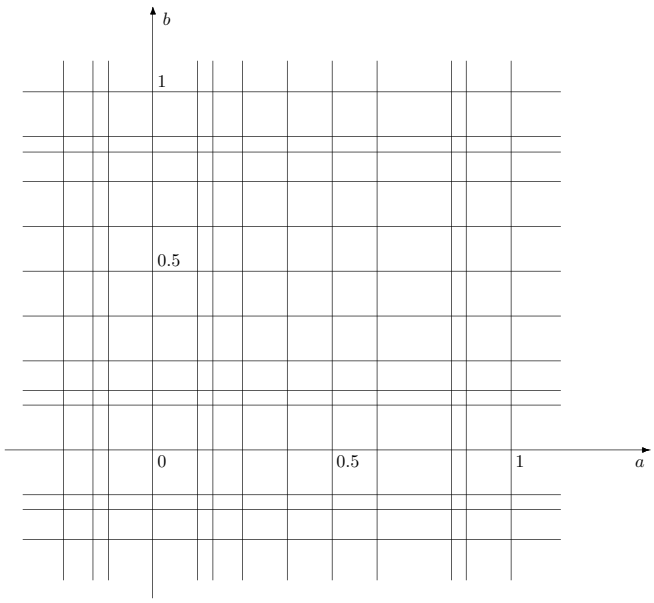

Figure 4.3: Parameter–plane grid for a direct–form filter with roundoff quantization after each multiplication and $B = 4$.

and the vertices need be considered separately. Therefore, in this case, the exhaustive analysis of a parameter region requires the consideration of: (i) one point inside each rectangle, (ii) one point for every side, and (iii) all vertices. The parameter plane grid for the two's complement truncation is similar to that for the magnitude truncation shown in Fig. 4.2.

Quantization after summation

When the quantizer is placed after summation as in (4.6), the indifference areas turn out to be convex polygons [10]. To understand this result with reference to the magnitude truncation quantization, consider the (a, b)–region leading from $[y(n-2) = j, y(n-1) = k]$ to $y(n) = i$,

which is defined by the following inequalities:

$$i \leq ak + bj < i + 1 \quad \text{for } i > 0, \tag{4.22}$$

$$-1 < ak + bj < 1 \quad \text{for } i = 0, \tag{4.23}$$

$$i - 1 < ak + bj \leq i \quad \text{for } i < 0. \tag{4.24}$$

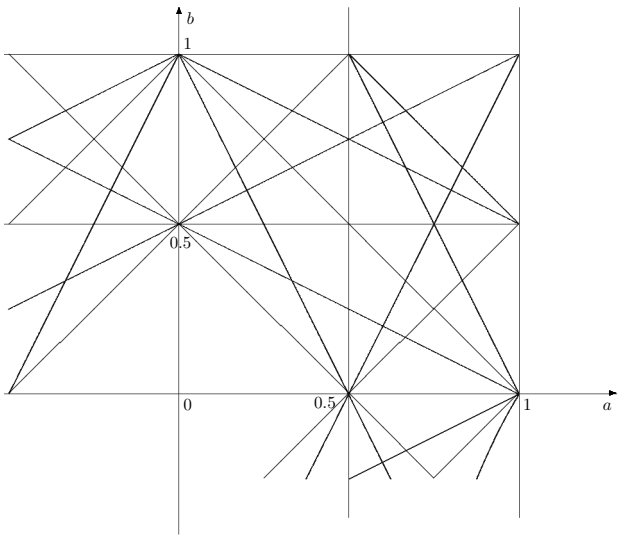

Figure 4.4: Parameter–plane grid for a direct–form filter with magnitude–truncation quantization after summation and $B = 2$.

Each of the above relations defines a stripe of the (a, b)–plane between parallel lines having slope equal to $-k/j$. Therefore, to draw the grid lines in the region where the output magnitude cannot exceed the upper bound B, it is necessary: (i) to consider the points $\pm|i/k|$ and $\pm(|i| + 1)/|k|$ on the a–axis and the points $\pm|i/j|$ and $\pm(|i| + 1)/|j|$ on the b–axis with $|j|, |k|, |i| \leq B$, and (ii) to connect each of the points on the a–axis with all of the points on the b–axis, excluding those for which the slope of the connecting straight line is different from $\pm|k/j|$ with $|j|, |k| \leq B$. In this way, the grid corresponding to $B = 2$ in the region $\mathcal{R} = \{(a, b) : 0 \leq a \leq 1, 0 \leq b \leq 1\}$ turns out to be the one shown in Fig. 4.4: there are 38 indifference areas in the first quadrant, but only 17 of these lie inside the stability triangle of the linear prototype.

The grid for the filter with one roundoff quantizer can be built according to a similar procedure, but the resulting indifference areas are more numerous, because the stripes to be considered in this case, that is:

$$i - \frac{1}{2} \leq ak + bj < i + \frac{1}{2} \quad \text{for } i > 0, \tag{4.25}$$

$$-\frac{1}{2} < ak + bj < \frac{1}{2} \quad \text{for } i = 0, \tag{4.26}$$

$$i - \frac{1}{2} < ak + bj \leq i + \frac{1}{2} \quad \text{for } i < 0, \tag{4.27}$$

determine a more closely–woven grid than that corresponding to inequalities (4.22).

The grid for the filter with one value truncation quantizer is again influenced by the asymmetry of the quantization characteristic. It is formed by the same lines as in the case of magnitude truncation with the addition of the straight lines through the origin having slope $\pm|k/j|$ with $|j|, |k| \leq B$. Moreover, the filter behaviour inside the indifference areas is different from that corresponding to each side and vertex. Note, however, that, due to the finite wordlength representation of a and b, not all of the points on the boundaries of the indifference areas can actually be attained.

4.4 Global asymptotic stability

The parameter plane partition illustrated in Section 4.3 can be used to find the *entire* parameter region where the digital filters with roundoff quantizers are globally asymptotically stable. This result cannot be achieved with the alternative methods suggested in the literature (cf., e.g., [11]).

Consider, for example, the filter (4.5) with two roundoff quantizers. This filter can be globally asymptotically stable only inside the octagonal region internal to the stability region of the linear prototype depicted in Fig. 4.5, because limit cycles have been detected outside it [15].
Above the parabola $a^2 + 4b = 0$, where the poles of the linear prototype are real, according to [16] the amplitude of the possible limit cycles cannot exceed $B = 3$.
Below the same parabola, where the poles of the linear prototype are complex, the bound on the limit cycle amplitude derived in [17] is $B = 2$.

To check stability, it is enough to test the filter behaviour only at the 16 points marked in Fig. 4.6.

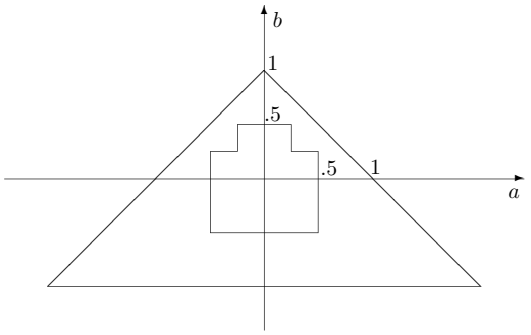

Figure 4.5: Stability region of the filter with two roundoff quantizers (after multiplications).

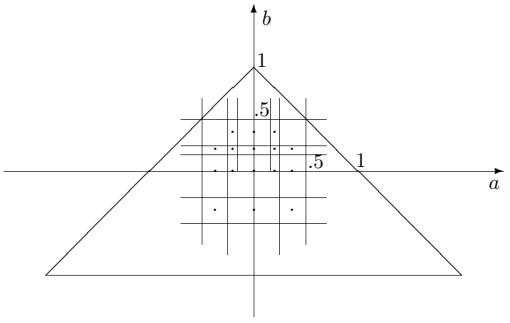

Figure 4.6: Minimal grid for cheking the stability of the filter with two roundoff quantizers.

Concerning the initial state $[y(-2), y(-1)]$, owing to the symmetry of the roundoff characteristic, it suffices to consider the pairs such that $1 \leq y(-1) \leq B$ and $|y(-2)| \leq y(-1)$. Moreover, if a trajectory leads to $|y(i)| > B$ for some i, the corresponding computation can be stopped since all of the trajectories starting from the considered initial states tend either to the origin or to a limit cycle with maximum amplitude less than B, so that the final part of the trajectories passing through $|y(i)| > B$ will be found starting from some other initial conditions

satisfying the bound. By performing the computations for the marked points, it is straightforward to verify that all of the trajectories converge to zero. Therefore, the filter is globally asymptotically stable all over the internal octagonal region shown in Fig. 4.5 (and only there).[1]

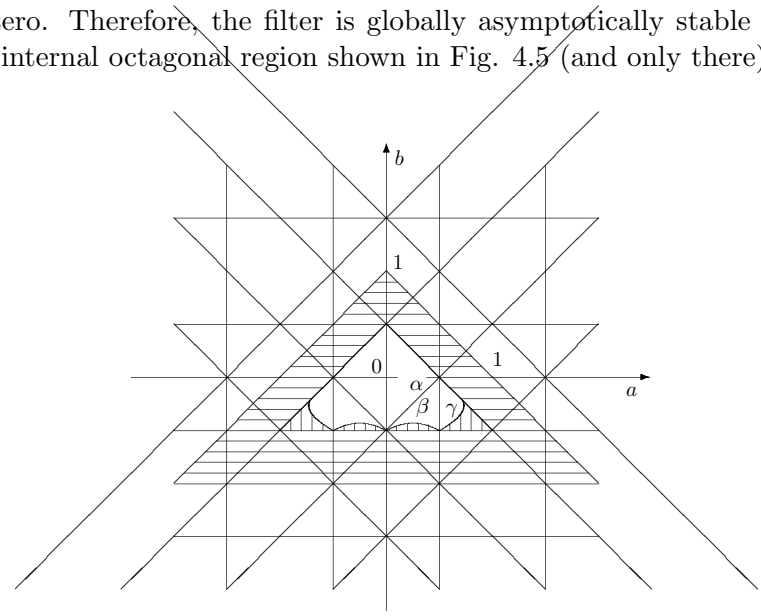

Figure 4.7: Stability region (unhatched and vertically hatched) of the filter with one roundoff quantizer after summation.

As another example, consider the filter (4.6) with one roundoff quantizer. According to previous literature, this filter exhibits limit cycles in the horizontally hatched region of Fig. 4.7, it is stable inside the unshaded region internal to the triangular stability region of its linear prototype, whereas no conclusion can be drawn concerning the vertically hatched region.

The method of the indifference areas shows instead that the filter is stable there, too. In fact, $B < 2$ inside the triangle defined by $-1/2 < b < 1/2 - |a|$. Therefore, it is enough to consider the coarse parameter grid shown in Fig. 4.7, and the analysis reduces to checking stability at a single point for each of the three triangular areas denoted by α, β and γ with initial conditions $[y(-2), y(-1)]$ equal to either $[1, 1]$ or $[0, 1]$. Anyway, since stability has already been proved for the entire region α and for parts of β and γ, stability is guaranteed also in the remaining parts of β and γ.

4.5 Existence area of a cycle

The method of the indifference areas can be applied to determine the entire region of the parameter plane where a given limit cycle is supported [12]. To this purpose it is enough to find the regions where every sequence of three consecutive output values in the cycle is supported. The region where the cycle is supported will be given by the intersection of the regions corresponding to all of these triplets.

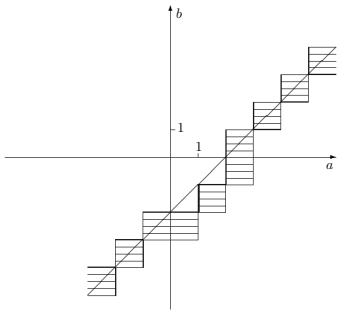

Figure 4.8: Region (shaded) where the sequence $\{-1, 1, 2\}$ of output values is supported by a direct–form filter with two magnitude–truncation quantizers (after multiplications).

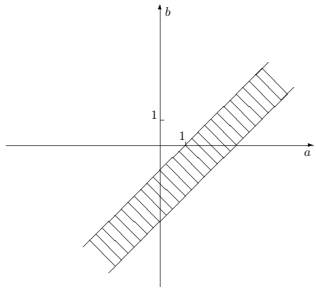

Figure 4.9: Region (shaded) where the sequence $\{-1, 1, 2\}$ of output values is supported by a direct–form filter with one magnitude–truncation quantizer (after the adder).

In the case of quantization after multiplication, the region supporting a sequence is formed by a family of rectangles whose diagonals lie on the

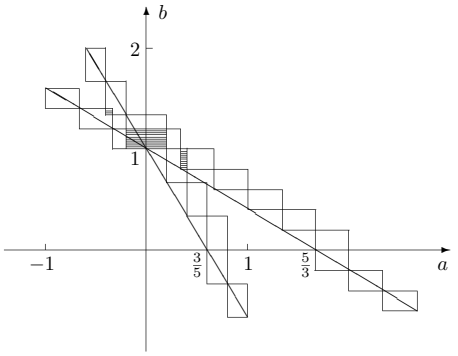

Figure 4.10: Existence area (shaded) of the limit cycle $\{3, 5\}$ for the filter with two magnitude–truncation quantizers (one after each multiplication).

same straight line within each quadrant, as shown in Fig. 4.8, whereas, in the case of quantization after summation, the region for the sequence is a stripe between slanted parallel lines, as shown in Fig. 4.9. In this way, if it is known that a cycle is sustained at a point, then it is possible to determine all of the points where the cycle can occur.

Fig. 4.10 shows the existence area of the cycle $\{3, 5\}$ for the filter with two magnitude–truncation quantizers. The cycles $\{-3, 5\}$ and $\{3, -5\}$ are possible in the areas symmetric about the b–axis to those represented in Fig. 4.10.

4.6 Concluding remarks

The method of the indifference areas allows us to find the entire parameter region where second–order digital filters are globally asymptotically stable as well as the regions where given limit cycles exist.

The method is effective and conceptually simple. Moreover, its computational complexity is less than that of alternative techniques that do not even ensure the exhaustive analysis of the region where the linear prototype is stable.

Bibliography

[1] M.J. Werter, *Suppression of Parasitic Oscillations due to Overflow and Quantization in Recursive Digital Filters*, Ph.D. dissertation, Eindhoven University of Technology, Eindhoven,The Netherlands, 1989.

[2] A.V. Oppenheim, R.W. Schafer, and J.R. Buck, *Discrete–Time Signal Processing* (2nd ed.), Prentice Hall, Upper Saddle River, NJ, 1999.

[3] B. Widrow and I. Kollar, *Quantization Noise: Roundoff Error in Digital Computation, Signal Processing, Control, and Communications*, Cambridge University Press, Cambridge, UK, 2008.

[4] V. Singh, "Stability analysis of a class of digital filters utilizing single saturation nonlinearity", Automatica, vol. 44, no. 1, pp. 282–285, 2008.

[5] V.Krishna Rao Kandanvli and H. Kar, "An LMI condition for robust stability of discrete–time delayed systems using quantization/overflow nonlinearities", Signal Processing, vol. 89, no. 11, pp. 2092–2102, 2009.

[6] R.A. Roberts and C.T. Mullis, *Digital Signal Processing*, Addison–Wesley, Reading, MA, 1987.

[7] P.K. Sim and K.K. Pang, "Decoupling of the overflow and quantization phenomena in orthogonal biquad recursive digital filters", Circuits Systems Signal Processing, vol. 6, no. 4, pp. 457–470, 1987.

[8] G. Amit and U. Shaked, "Small roundoff noise realization of fixed–point digital filters and controllers", IEEE Trans. Acoust. Speech Signal Process., vol. ASSP–36, no. 6, pp. 880–891, 1988.

[9] A. Lepschy, G.A. Mian, and U. Viaro, "Parameter space quantization in fixed–point digital filters", Electron. Lett., vol. 22, no. 7, pp. 384–386, 1986.

[10] A. Lepschy, G.A. Mian, and U. Viaro, "Parameter plane quantization induced by the signal quantization in second–order fixed–point digital filters with one quantizer", Signal Processing, vol. 14, no. 1, pp. 103–106, 1988.

[11] K.T. Erickson and A.N. Michel, "Stability analysis of fixed–point digital filters using computer generated Lyapunov functions - Part I: Direct form and coupled form filters", IEEE Trans. Circuits Syst., vol. CAS–32, no. 2, pp. 113–132, 1985.

[12] A. Lepschy, G.A. Mian, and U. Viaro, "Limit cycles due to the signal quantization in digital filters", Atti Ist. Veneto SS.LL.AA., Tomo CXLVI: Classe di Scienze Fisiche, Matematiche e Naturali, pp. 1-19, 1988.

[13] U. Viaro, *Twenty-Five Years of Research with Antonio Lepschy*, Edizioni Libreria Progetto, Padova, Italy, 2009.

[14] B.D. Green and L.E. Turner, "New limit cycle bounds for digital filters", IEEE Trans. Circuits Syst., vol. CAS–35, no. 4, pp. 365–374, 1988.

[15] L.B. Jackson, "An analysis of limit cycles due to multiplication rounding in recursive digital (sub)filters", Proc. 7th Allerton Conf. Circuit System Theory, pp. 69–78, 1969.

[16] J.L. Long and T.N. Trick, "An absolute bound on limit cycles due to roundoff errors in digital filters ", IEEE Trans. Audio Electroacoustics, vol. AU–21, no. 1, pp. 27–30, 1973.

[17] Z. Ünver and K. Abdullah, "A tighter practical bound on quantization errors in second–order digital filters with complex conjugate poles", IEEE Trans. Circuits Syst., vol. CAS–22, no. 7, pp. 632–633, 1975.

Often, short papers tend to be sharper than longer works because they focus on a single theme without lingering on unessential aspects, thus showing clearly the signicance of a contribution or an idea. The author of this book had the privilege of collaborating for over a quarter of a century with Antonio Lepschy (1931-2005), a recognized leader of the Italian control community.

Lepschy had a liking for the brief paper format, so that many results obtained by his research team were published in this way. The present compilation tells a few of these short stories, duly updated, trying to preserve their original flavour.

Umberto Viaro (http://umbertoviaro.blogspot.com/) has been professor of System and Control Theory at the University of Udine, Italy, since 1994. His 25-year-long collaboration with Antonio Lepschy resulted in more than 100 joint papers and two books. An essential role in this research activity was played by Wiesław Krajewski of the Systems Research Institute, Polish Academy of Sciences. The current research interests of Umberto Viaro concern optimal model reduction, robust control, switching and LPV control. He is the author or coauthor of 4 books and about 180 research papers.

ISSN 0208-8029
ISBN 9788389475282

SYSTEMS RESEARCH INSTITUTE
POLISH ACADEMY OF SCIENCES
Phone: (+48) 22 3810246 / 22 3810241 / 22 3810273
tel. (22) 3810 277; e-mail: biblioteka@ibspan.waw.pl